Transactions on Electrical and Electronic Materials
https://doi.org/10.1007/s42341-024-00525-4

Online ISSN 2092-7592
Print ISSN 1229-7607

REGULAR PAPER

Experimental Studies of Bimetallic Zinc-Cadmium Admixed L-Threonine Single Crystal

M. Abila Jeba Queen[1] · K. C. Bright[2] · P. Aji Udhaya[1]

Received: 11 September 2023 / Revised: 7 February 2024 / Accepted: 18 February 2024

Abstract
A bimetallic compound Zn^{2+} [Cd $(C_2H_3O_2)$ $(C_4H_8NO_3)$ (H_2O)], fabrication and its analysis is the major focus of this article. The bimetallic single crystal namely Zinc L-threonine Cadmium Acetate, has been crystallized by the simple method of slow evaporation technique. X-ray diffraction technique identified that, the prepared bimetallic single crystal with asymmetric units of a polymeric structure belongs to the class of monoclinic crystal system with a=5.87 Å, b=8.87 Å, c=10.81 Å, α=γ=90°, β=91.84°, space group $P2_1$ and volume 563Å^3. The optical nature of the crystal specifically its transparency has sufficiently increased nearly cent percentage due the presence of organic ligand's present in the L-threonine amino acids. The impacts of zinc on the thermal stability and different stages of chemical degradations are studied with the aid of Thermo gravimetric and differential thermal analysis. Thermal stability increases nearly 5% with the addition of zinc concentration. The dielectric studies support the finding that the zinc doping increases dielectric constant by five times compared to the L-threonine cadmium acetate crystal. Second harmonic generations efficiency increases almost 20% in each 0.2 mol% of the zinc addition. Magnetic properties are also elucidated and the effect of zinc has been analysed and the materials are identified as a paramagnetic nature due to the partially filled electron in the d-shell of Zn^{2+}ion.

Keywords Paramagnetic · Bimetallic · Organocadmium · Red shift

1 Introduction

Organometallic compounds with immense group of chemical substance which are important to the materials research. Metal with organic moiety have a notable structural, optical magnetic and dielectric properties mainly due to one or several organometallic fragments are connected to a conjugated system [1]. Metal with organic moiety belongs to the general class of coordination compound and a host of such compounds with majority metals have synthesized with a wide variety of organic substrate [2]. Organocadmium compounds react only with acids; the reactions are limited due to the fact that only primary alkyl cadmium compounds are stable. Cadmium has relatively large polarisable ion due to completely filled 4d shell results to high affinity for electron donors [3]. L-Threonine cadmium acetate monohydrate compound has been identified as an excellent material with the wide applications in the field of medicine, chemical precursor, corrosion preventers in electronic products and optoelectronic device fabrications [4–6]. Zinc acetate is a semiconductor element has the advantage of wide band gap, large free exciton binding energy, high carrier mobility, high transparency, wide range resistivity and excellent photoelectric, piezo electric, thermoelectric properties it was utilized as a preservation, dye mordant, additives, light industry, radiation protection, gas sensors, Infra Red (IR) detectors and photodiodes. The main important application of zinc is used in nuclear power plants as a plating inhibitor on primary water piping [7]. L-threonine is a neutral amino acid, which is dipolar in nature with isoelectric point 5.60 [8].

The synthesized and the characterization of L-threonine cadmium acetate monohydrate had been reported previously. The structure has identified as a typical layered supra molecular organization. Within the layered structure, each cadmium ion has liked with six oxygen coordination environments. The cadmium sites are connected through common faces, which involves longer cadmium–oxygen distances (2. 475 Å) and through common edges of cadmium–nitrogen distance (2.274 Å) [9, 10]. The physical and the chemical properties of the materials had tuned by adding the compounds such as univalent potassium ions [11] and the bivalent lead ions

✉ M. Abila Jeba Queen
jeba.abi@gmail.com

[1] Department of Physics, Holy Cross College (Autonomous), Nagercoil, Tamil Nadu 629004, India

[2] Department of Physics, Mar Ivanio's College (Autonomous), Thiruvananthapuram, Kerala 695015, India

Published online: 28 March 2024

[12] which is highly suitable for prism fabrication with good magnetic behaviour. With the objective that like other metals like lead and potassium, zinc also alter the materials physico chemical properties especially its non linear optical response. The research gap identified here is that, nobody reported the effect of zinc on the L- threonine cadmium acetate crystal. Now it is decided to study the effect of zinc (Zn^{2+}) ions on the optical, electrical and magnetic properties of L-threonine cadmium acetate and the results are reported in this paper.

2 Experimental Methods

Zinc L-threonine Cadmium Acetate single crystals were crystallised by incorporating 0.2, 0.4 and 0.6 mol% of zinc acetate dihydrate into the equal molar solution of L-threonine and cadmium acetate. L-threonine cadmium acetate solution is prepared by taking the one molar L-threonine and one molar cadmium acetate which was completely mixed with 50 ml of distilled water. The saturated solution has been formed by continuous stirring and heating about ten hours at an ambient pressure. To the saturated solution X molar (X = 0.2, 0.4 and 0.6 mol%) zinc acetate dehydrate was added separately and mixed continuously using the magnetic stirrer. After the continuous stirring the solution was heated 40° C about an hour thus the homogeneous solution is obtained. At this condition the solvent evaporates and solid mixture obtained. The synthesised solid mixture was re-crystallized twice and then the solution was kept in the constant temperature bath at a temperature $35 \pm 2\,^{\circ}C$. Nucleation takes place after 9 days and good quality ZLTCA single crystals synthesized within a period of 40 days. The photograph of ZLTCA single crystals are shown in Fig. 1. The chemical reaction takes place during the crystallization process is as follows:

$$Cd(CH_3COO)_2.2H_2O + C_4H_9NO_3 \rightarrow [Cd(C_2H_3O_2)(C_4H_8NO_3)(H_2O)]H_2O$$

$$[Cd(C_2H_3O_2)(C_4H_8NO_3)(H_2O)]H_2O + X[Zn(CH_3COO)_2(H_2O)_2] \rightarrow X[Zn^{2+}[Cd\ (C_2H_3O_2)\ (C_4H_8NO_3)\ (H_2O)]]$$

3 Result and Discussion

The effect of zinc addition on the lattice structure of LTCA has identified for 0.4 mol% of zinc ions added L-Threonine Cadmium Acetate single crystals were carried out with aid of Bruker Kappa APES II single crystal X-ray diffractometer using MoKα (λ = 0.71073 Å) radiations. The computed X-ray diffractometer results elucidates the unit cell parameters that, ZLTCA crystal belongs to monoclinic crystal system category and the lattice parameters are a = 5.87 Å, b = 8.87 Å, c = 10.81 Å, α = γ = 90°, β = 91.84°, space group $P2_1$ and volume 563 $Å^3$. LTCA also belongs to the same monoclinic crystal system but while adding the zinc which in turn brings changes in the lattice parameters, crystallographic axis and volume of the unit cell [9, 10].

The crystalline nature and phase identifications of the fabricated single crystals were analysed by identifying the crystalline planes of the diffraction pattern. The powder X-ray diffraction pattern of grown ZLTCA crystalline powder has been recorded with PAN alytical X'Pert Pro powder X-ray diffractometer operating at 40 kV and 30 mA, using copper target. The intensity data's are recorded by the continuous scanning with the scan step time of 10.16 s and scan size of 0.05°. The miller indices of all the obtained diffracted peaks are indexed by means of INDEXING software package given in Fig. 2. From the XRD diffraction pattern of all the three crystals, it was noticed that the predominant peaks correspond to (0 0 2) and (0 0 3) plane with the small variation in the degree of the peak positions. The sharp peaks of ZLTCA confirm the good crystalline nature of the crystallised material. Furthermore it was also noticed that the addition of Zn^{2+} leads to a change in the intensity of peaks with a slight shift in the peak positions.

Using the miller indices, the unit cell parameters of 0.2 and 0.6 mol% zinc added L-threonine cadmium acetate crystals were computed using the 'UNIT CELL' software package and are tabulated in Table 1. In comparison with the LTCA spectra [10], zinc doped L-threonine cadmium acetate shows variation in the diffracted peak intensity which arises due to the influence of zinc ions on the crystal system. Thus a fractional mole percentage of zinc addition creates

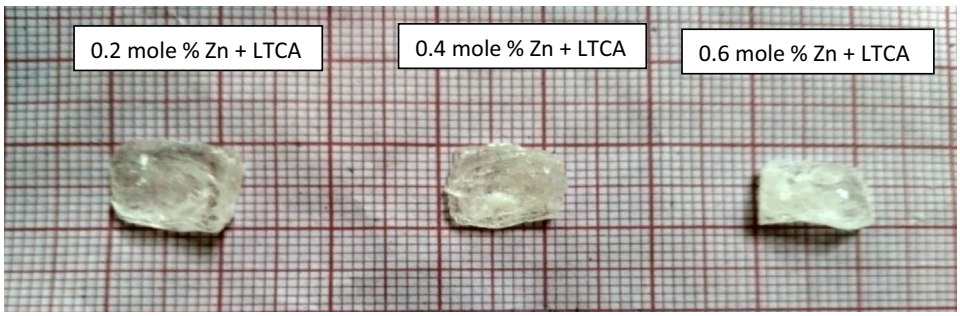

Fig. 1 Photograph of ZLTCA single crystals

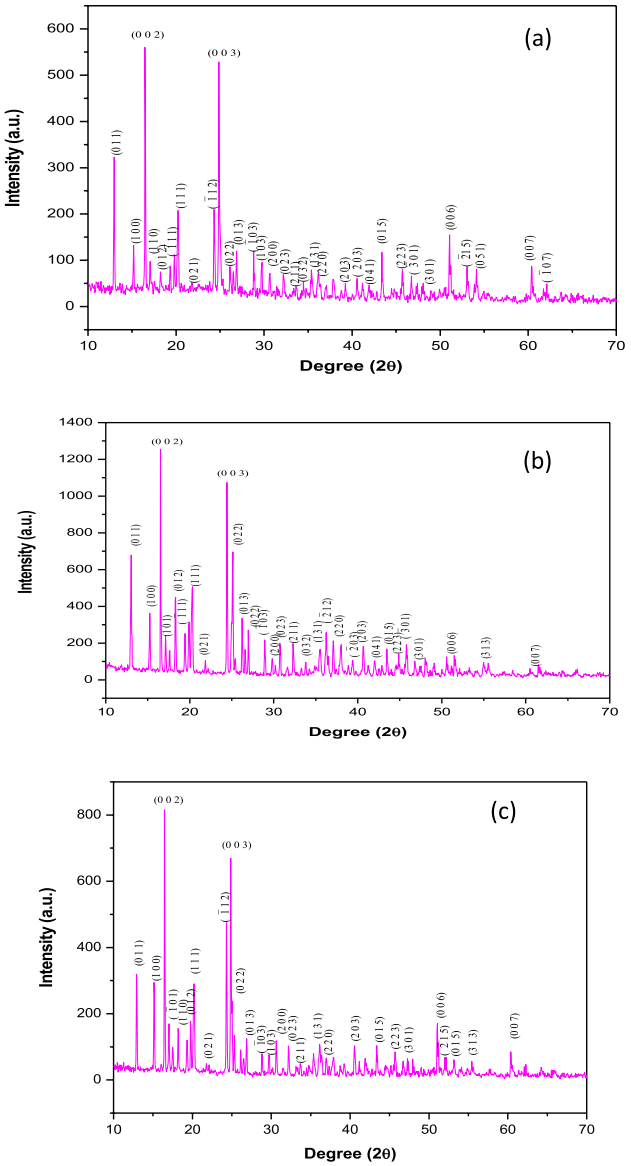

Fig. 2 Powder X-ray diffraction pattern **a** 0.2 mol% ZLTCA **b** 0.4 mol% ZLTCA **c** 0.6 mol% ZLTCA

changes in the internal structure of the crystal system; this was proved by the slight change in lattice parameters. Therefore from the analysis it was concluded that, there is no change in the crystal system of zinc cadmium threonine and remain in the monoclinic system, but the zinc atoms were successfully incorporated into the lattice of LTCA the same behaviour was already reported in the case of lead and potassium [11, 12].

Optical properties of the grown crystals are interrelated with the materials atomic structure, electronic band structure and electrical properties [13]. The optical transmittance spectrum of the ZLTCA crystals was recorded in the spectral range between 190 and 1100 nm using ELICO model UV spectrophotometer and is displayed in Fig. 3. It was observed that 0.2, 0.4 and 0.6 mol% of zinc L-threonine cadmium acetate crystals experiences a lower cut-off wavelength of 230 nm, 239 nm and 240 nm respectively. Thus zinc concentration improves the optical transmittance and also the cut off wavelength of the light extends towards the red region. The increase in transmittance percentage with respect to the concentration may be attributed due to fact that the addition of zinc leads to change in the bond length between the $\pi \rightarrow \pi^*$ transition.

The optical band gap calculation at the lower cut off wavelength (λ) determines the materials category and was calculated using the relation contains Plank's constant (h) and velocity of light (c) [14]:

$$\mathrm{Eg} = \frac{hc}{\lambda} \tag{1}$$

The grown 0.2, 0.4 and 0.6 mol% of zinc L-threonine cadmium acetate crystals have optical band gaps of 5.184 eV, 5.384 eV and 6.41 eV respectively at the particular lower cut off wavelength. Band gap calculation reveals that all the three crystals are best dielectrics. Due to its higher transmittance percentage and the red shift ZLTCA crystals can be used as optoelectronic devices. Moreover the monoclinic crystal system with higher transmittance percentage can be recommended for the prism fabrication.

The FTIR spectrum of ZLTCA crystalline powders were recorded with Perkin Elmer spectrometer using potassium bromide pellet technique and the recorded spectrums are given in Fig. 4. In this study, the vibrational analysis of the ZLTCA were performed based on the vibrations of threonine ions consist of amino group NH^{3+}, a carboxyl group COO^{-}, methyl group CH_3^{+}, hydroxyl groups and the acetate ions present in zinc and cadmium. The vibrational bands/peaks and their assigned peaks are depicted in Table 2. The ligands act as a absorbent and stabilize the functional head group

Table 1 Computed lattice parameters

Crystal name	Unit cell parameters	Crystal system	Space group	Volume (Å^3)
0.2 mol% Zn^{2+} added LTCA	a = 5.8415 Å, b = 9.0188 Å, c = 10.8152 Å α = γ = 90°, β = 94.1164°	Monoclinic	$P2_1$	568.3078
0.6 mol% Zn^{2+} added LTCA	a = 5.8331 Å, b = 8.87496 Å, c = 10.8503 Å α = γ = 90°, β = 93.3331°	Monoclinic	$P2_1$	552.8371

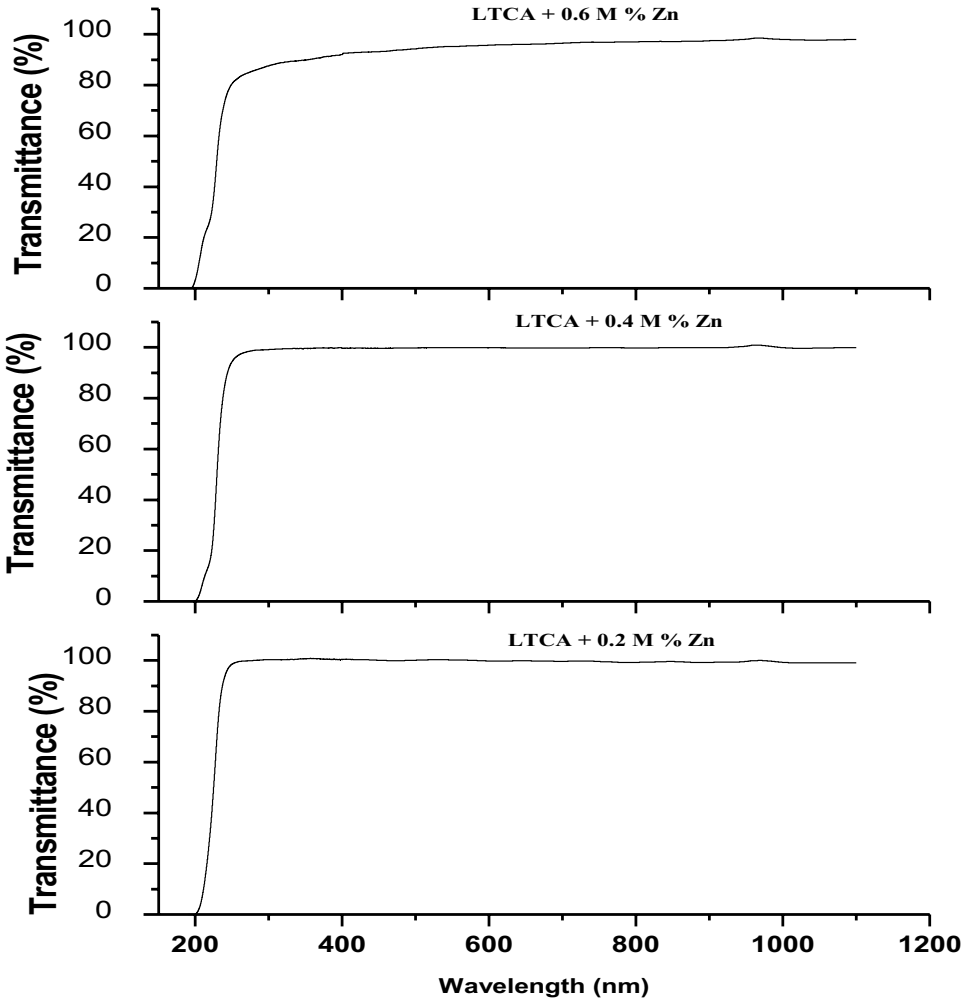

Fig. 3 UV Transmittance spectrum of ZLTCA crystals

and more hydrocarbon large groups they play a vital role in the control of nucleation and growth [15–18].

The broad vibrational band observed around 3400 cm^{-1} is assigned to the symmetric stretching mode of water molecules but in LTCA [11] the broad band observed at 3431 cm^{-1}. Small peak around 2900 cm^{-1} is identified as C-H asymmetric stretching vibrations of CH_3 group present in the threonine amino acid. The broad band around 2300 to 2500 cm^{-1}due to O = C = O group. Combinations of overtone bands exist in the frequency range between 2085 and 2144 cm^{-1}. CH_3 asymmetric stretching and bending vibrations are confirmed by the strong peak at 1570 cm^{-1} and 1350 cm^{-1}, 1415 cm^{-1} respectively. In LTCA the same peaks are observed at 1417 and 1354 cm^{-1} due to CH_3 asymmetric bending vibrations. The peak located near 1114 to 1190 cm^{-1} is attributed due to rocking of NH_3. In plane and out of plane CH_3 rocking modes appears near 1080 and 1001 cm^{-1} respectively, same rocking vibrations are found in LTCA at 1083 and 1001 cm^{-1}. The medium band near 1040 is identified as CN stretching and 900 cm^{-1} is due to CC stretching of ZLTCA whereas the same band observed at1039 cm^{-1} in LTCA with CN stretching. Additional peaks located near 840 cm^{-1}, 760–795 cm^{-1}, 550 and 620 $cm^{-1}$are assigned as CCN stretching, COO torsion, COO rocking and in plane OCO rocking respectively which is mainly due to the addition of the zinc acetate. In addition to the above, OCO symmetric bending and NH_3 torsion vibrations are identified due to the medium peaks present in the spectrum near 670 and 490 cm^{-1}. Furthermore the addition of zinc acetate leads to small change in the position of various bands and peaks the additional peaks such as CCN stretching, COO torsion, COO rocking and in plane OCO rocking arises due to the acetate molecules present in the compound.

The TG/DTA curve of zinc L-threonine cadmium acetate crystal is illustrated in Fig. 5. The first stage of

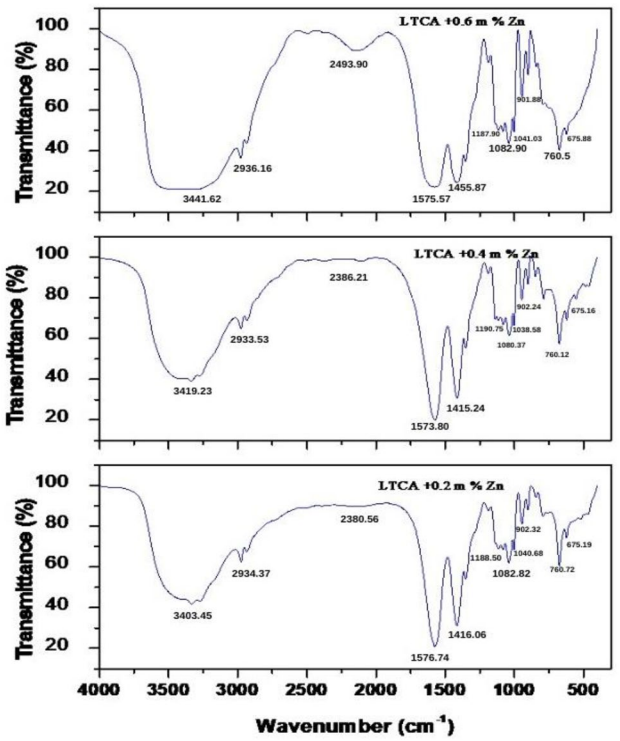

Fig. 4 FTIR spectrum of ZLTCA

Table 2 Spectral assignment of ZLTCA

Wavenumber (cm^{-1})			Assignment
0.2 mol% Zn + LTCA	0.4 mol% Zn + LTCA	0.6 mol% Zn + LTCA	
3403.45	3419.23	3441.62	O–H stretching of H_2O
2934.37 2976.13	2933.53 2976.74	2936.16 2977.99	C-H asymmetric stretching
2380.56	2386.21	2493.90	O = C = O stretching
2085.25	2097.29	2144.17	Combination and overtone bands
1576.74	1573.80	1575.57	CH_3 asymmetric stretching
1416.06 1352.23	1415.24 1351.92	1455.87 1353.86	CH_3 asymmetric bending
1188.50 1114.89	1190.75 1139.11 1115.49	1187.90 1139.2 1115.33	Rocking of NH_3
1082.82	1080.37	1082.90	Out of plane CH_3 rocking
1040.68	1038.58	1041.03	CN stretching
1001.58	1001.84	1001.87	In plane CH_3 rocking
944.36 902.32	945.78 902.24	945.10 901.88	CC stretching
846.07	849.83	843.92	CCN stretching
793.19 760.72	790.11 760.12	792.84 760.5	Torsion of COO
675.19	675.16	675.88	OCO symmetric bending
622.72	621.40	623.65	Out of plane OCO rocking
523.25	555.57	555.35	COO rocking
485.85	485.32	–	NH_3 torsion

decomposition is dehydration and the first stage of weight loss around 11% observed which corresponds to loss of two water molecules. The second stage of weight loss about 7% is due to the liberation of two carbon molecules. Both the weight losses are experienced for all the three samples. Further, as can be discerned from the TG curve, third stage of decomposition occurs around 200 °C corresponds to the weight loss of 38, 36 and 35% respectively for 0.2, 0.4 and 0.6 mol% of zinc added L-threonine cadmium acetate. Final weight loss of 10 and 11% observed for the 0.2, 0.4 and 0.6 mol% of zinc added LTCA respectively. It is noted that there is good agreement with calculated and observed weight loss. TG weight loss curve coincides with the obtained TGA curve. For 0.2 mol% of zinc added LTCA the exothermic peaks at 128.20, 202.72, 298.52 and 623.59 °C corresponds to the liberation of two molecules of water, two molecules of carbon, $C_4H_{13}NO_3$ and CH_3O respectively. Exothermic peak at 130.01, 195.93 and 316.13° C for 0.4 mol% of zinc added LTCA corresponds to the decomposition of $2H_2O$, 2C and $C_4H_9NO_3$ respectively. Furthermore, 0.6 mol% of zinc shows exothermic peak at 124.94, 204.95, 294.77 and 583.81 due to the $2H_2O$, 2C, $C_4H_7NO_3$ and CH_9O liberation. From the thermal analysis it was confirmed that the thermal stability of the zinc added materials enhances, the thermal stability of parent compound is 105° C whereas the stability of zinc added LTCA is 130 °C. As the zinc concentration increases the thermal stability of the material is increases which are mainly due to the role of zinc atoms in the materials.

To understand the dielectric properties of the grown crystal, the effect of frequency on dielectric constant and dielectric loss was studied and the variations are plotted as shown in Figs. 6 and 7 respectively. Dielectric constant graph witness that for all the three crystals, dielectric constant increases with increase in temperature but decreases with increase in frequencies. Higher values of dielectric constant experienced at higher temperature and lower frequencies.

For 0.2 mol% of ZLTCA crystal, dielectric constant decreases with increase in temperature. Same behaviour was experienced in the case of two frequencies like 1 kHz and 10 kHz. Maximum value of dielectric constant obtained at lower temperature and frequencies. For other frequencies such as 100 kHz, 1 MHz and 1 MHz dielectric constant and dielectric losses are almost same for

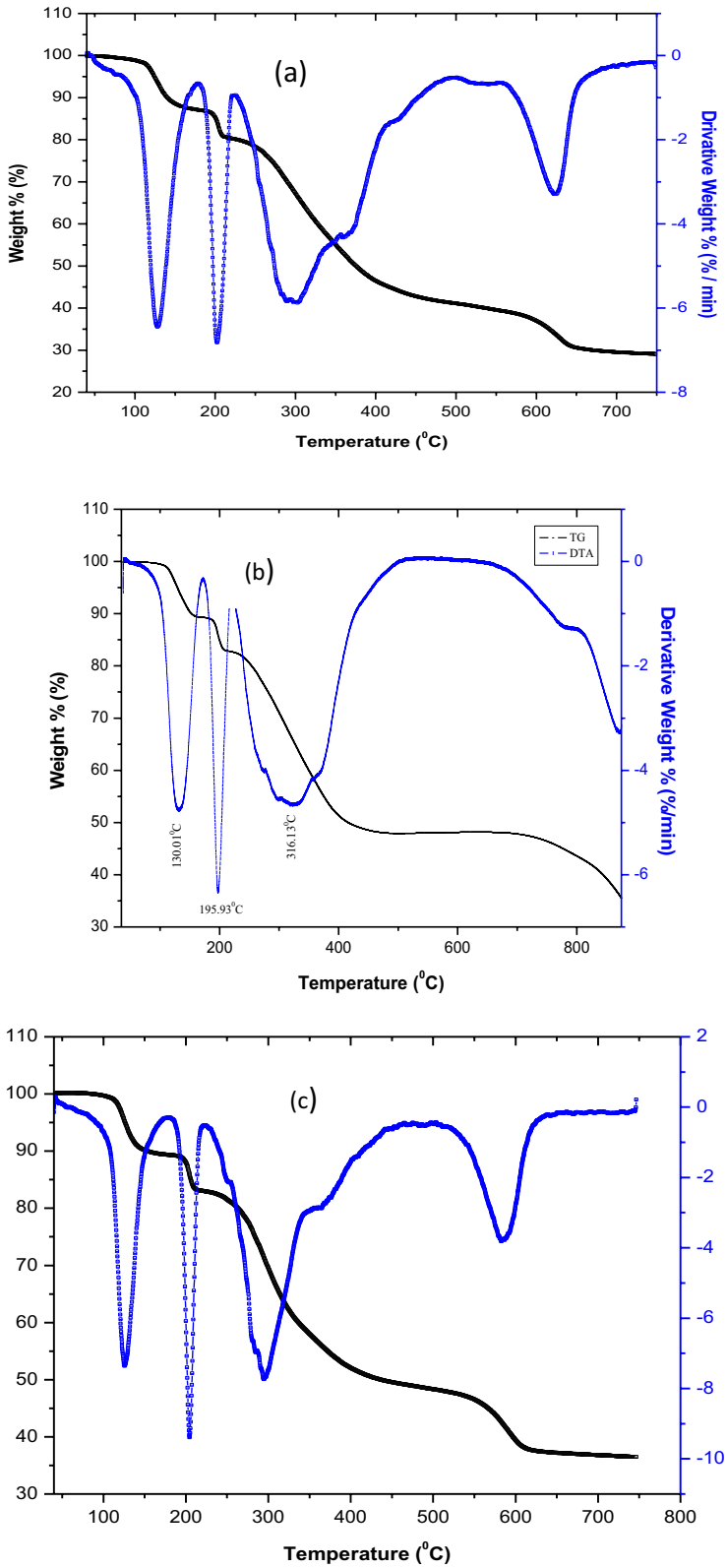

Fig. 5 TG / DTA curve **a** 0.2 mol% of zinc LTCA **b** 0.4 mol% of zinc LTCA **c** 0.6 mol% of zinc LTCA

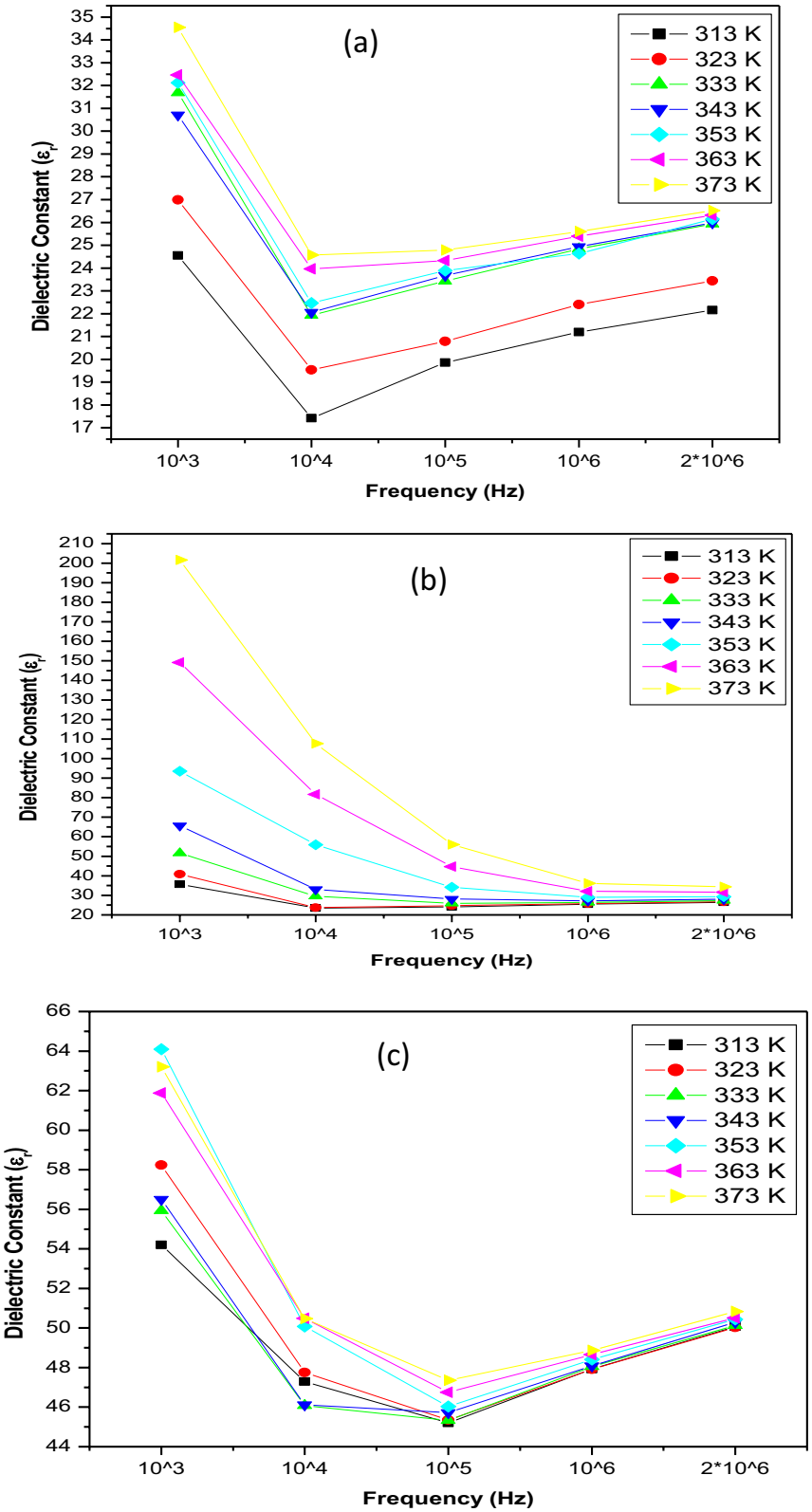

Fig. 6 Dielectric constant **a** 0.2 mol% of zinc LTCA **b** 0.4 mol% of zinc LTCA **c** 0.6 mol% of zinc LTCA

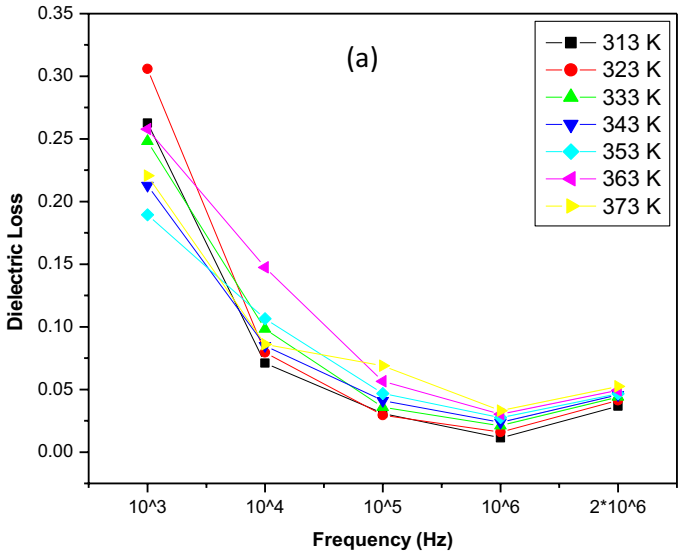

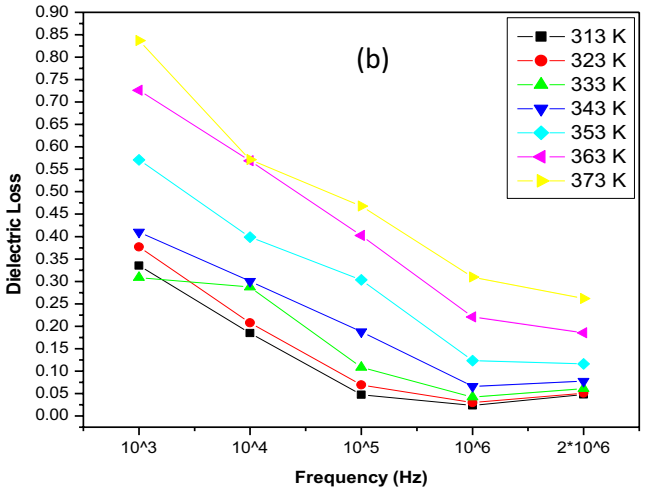

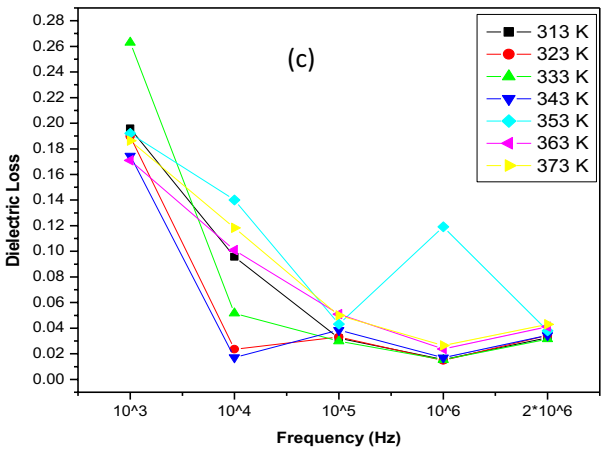

Fig. 7 Dielectric loss **a** 0.2 mol% of zinc LTCA **b** 0.4 mol% of zinc LTCA **c** 0.6 mol% of zinc LTCA

all the temperatures. As the frequency increases, dielectric constant decreases. Dielectric loss of 0.2 mol% of ZLTCA crystal increases with increase in temperature and decrease with increase in frequency. For 0.4 mol% ZLTCA crystal, dielectric constant and dielectric loss increases with increase in temperature and decrease with increase in frequency. The maximum value of dielectric constant obtained at 373 K temperature and 1 kHz frequency.0.6 mol% of ZLTCA crystal maximum value of dielectric constant at 373 K temperature and 1 kHz frequency. The dielectric constant and dielectric loss of the crystal increases with increase in temperature and decrease with increase in frequency. The synergistic effect of the zinc ions can boost the electrochemical property of the material which can be utilizes as a super capacitor applications [19]. For the lower frequency, the higher value of dielectric constant arises due to the fact that large numbers of space charge polarizations. As the input frequencies are increases the polarisation decreases. Further increases in frequency, eliminates the polarization near grain boundaries and then the dielectric constant enhances because of the zinc and the cadmium ions [20].

The second harmonic generations (SHG) of ZLTCA crystals were determined by modified technique of Kurtz and Perry [21]. The second harmonic output was generated by irradiating the powder sample by a pulsed laser beam. The LASER source is generated at a wavelength of 1064 nm from Neodymium-doped Yittrium Aluminium garnet (Nd-YAG) laser with a pulse width of 6 ns and pulse energy of 0.70 J and repeatation rate of 10 Hz. The SHG output voltage of reference Potassium Dihydrogen Phosphate (KDP) is 8.94 mV and the relative SHG efficiency of the doped samples are tabulated in Table 3. From the table it was known that the SHG efficiency of the ZLTCA enhances as the concentration of zinc increases. This is attributed due to two reasons: the variation in the electronic configuration of cadmium and zinc metals. Cd^{2+} and Zn^{2+} ionic configurations are $3d^{10}$ and $4s^2$ respectively. Secondly zinc has lesser ionic radius compared to cadmium [22] as a result the zinc addition increases the SHG efficiency. Due to the lower electron affinity of the ZLTCA, the material can be considered as a good candidate for NLO phenomenon [23–25].

Table 3 Comparison of SHG efficiency of ZLTCA with KDP

Crystal	Output power (mV)	SHG efficiency (%)
KDP	8.94	100
0.2 mol% Zn + LTCA	4.25	47.5
0.4 mol% Zn + LTCA	5.63	62.9
0.6 mol% Zn + LTCA	7.37	82.4

The magnetic field versus moment curve for the ZLTCA samples are depicted in Fig. 8 and their corresponding magnetic parameters are tabulated in Table 4. The Field Moment (M-H) curve confirmed that the ZLTCA shows paramagnetic nature due to the partially filled electron in the d-shell of Zn^{2+}ion and the total spin is non zero value. When an external magnetic field is applied, the electron spins to align the direction parallel to the applied field.

From the table, it is noted that the saturation magnetization increases for all the zinc doped samples due to the incorporation of the zinc. The ZLTCA materials possess permanent dipoles, in the absence of external magnetic field the dipoles orient themselves. Thus the net magnetization of ZLTCA in any direction is zero. When the magnetic field is applied, it attracts the magnetic lines of forces which tend to enhance the saturation magnetization value. Magnetic properties changes due to the addition of zinc (0.74 Å) with lower ionic radius compared to cadmium (0.95 Å) metal. The magnetic moment of the ZLTCA material is calculated as 8.944 Bohr Magneton, since zinc and cadmium compounds have no unpaired electrons paramagnetic nature arises because of the carbon, hydrogen, nitrogen and oxygen present in the compound.

4 Conclusion

A bimetallic compound zinc-cadmium admixed L-threonine single crystals were crystallized by evaporation method at the ambient temperature and pressure. The polymeric structure of the compound with the monoclinic crystal system is suitable for optical device fabrications especially for prism fabrication. The poor absorption ability might be used as a corrosion resistant semiconductor material and sunscreen applications due to its high percentage of transmittance. Thermal stability increases due to the addition of the zinc metal. Dielectric studies reveal that, metals with more electropositive character of zinc improves the dielectric property which again tolerance to the semiconductor nature of the material. The static permittivity enhances due to the hopping agent of Zn^{2+} and Cd^{2+}. The dielectric property tuned by the Zn^{2+} doping can be used as a gate dielectrics for organoic transistor, organic capacitors and a corrosion inhibitor for optical device fabrications. The M-H curve depicts that the magnetic behaviour changes by adding zinc, crystal shows paramagnetic nature this can be used as a biocompatibility in various tissue engineering applications that permits to image biomedical application, magnetic image experiments, switching and magnetic storage.

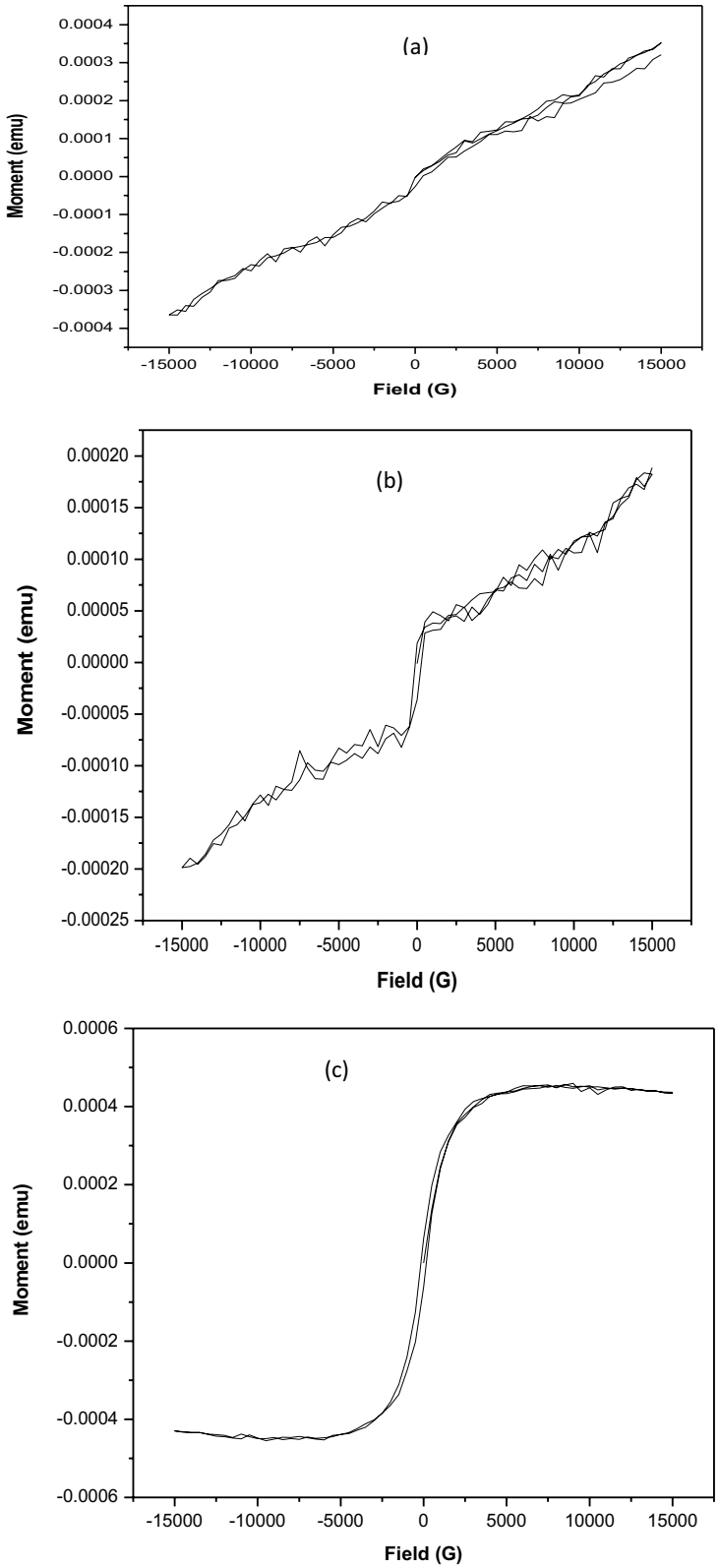

Fig. 8 Field Moment graph **a** 0.2 mol% of zinc LTCA **b** 0.4 mol% of zinc LTCA **c** 0.6 mol% of zinc LTCA

Table 4 Magnetic parameters of ZLTCA

Name of the samples	Coercivity (HC) (G)	Retentivity (E^{-6} emu)	Magnetization (E^{-6} emu)
LTCA + 0.2 mol% Zn^{2+}	197.80	27.410	193.68
LTCA + 0.4 mol% Zn^{2+}	257.85	20.795	275.52
LTCA + 0.6 mol% Zn^{2+}	457.19	62.031	164.70

Author Contributions All the authors contributed equally to the study, conception, design and all the authors commented on the previous versions of the manuscript. All the authors read and approved the final manuscript.

Funding Not applicable.

Data Availability The datasets generated during and/or analysed during the current study are available from the corresponding author on reasonable request.

Declarations

Conflict of Interest The authors declares that no conflict of interest.

Ethical Approval This article does not contain any studies involving human participants or animals performed by any of the authors.

Informed Consent Statement Not applicable.

References

1. G.D. Batema, C.A. van Walree, G.P.M. van Klink, C. de Mello Doneg, A. Meijerink, J. Perez-Moreno, K. Clays, G. van Koten, Octupolar organometallic Pt(II) NCN-pincer complexes; synthesis, electronic, photophysical, and NLO properties. J. Organomet. Chem. **867**, 246–252 (2018)
2. C.P. Raptopoulou, Metal organic frameworks synthetic methods and potential applications. Materials (Basel) **14**, 310 (2021)
3. S.K. Tilley, R.C. Fry, *Systems biology in toxicology and environmental health* (Elsevier, Academic Press, 2015)
4. A. Roy Chowdhury, R. Datta and D. Sarkar, Heavy Metal Pollution and Remediation, ed. by B. Torok, T. Dransfield (Elsevier, Academic Press, 2018)
5. E.W.P. Wong, C.Y. Cheng, *Comprehensive toxicology* (Elsevier, USA, 2010)
6. Pathaik and Pradyot, *Handbook of inorganic chemical compounds* (Mcgraw Hill Professional, New York, 2003)
7. H.C. You, Transistor characteristics of zinc oxide active layers at various zinc acetate dihydrate solution concentrations of zinc oxide thin-film. J. Appl. Res. Technol. **13**, 291–296 (2015)
8. R.L. Madan, *Organic chemistry* (Tata McGrew Hill Education private Limited, New Delhi, 2013)
9. M. Abila Jeba Queen, K.C. Bright, S. Mary Delphine, catena-Poly [[[(acetato-κ2O, O′)aquacadmium(II)]-μ-L-threoninato-κ3N, O:O′]monohydrate]. IUCr Data **3**, x181770 (2018). https://doi.org/10.1107/S2414314618017704
10. M. Abila Jeba Queen, K.C. Bright, S. Mary Delphine, P. Aji Udhaya, Spectroscopic investigation of supramolecular organometallic compound L-threonine cadmium acetate monohydrate. Spectrochim. Acta A Mol. Biomol. Spectrosc. **228**, 117802 (2019). https://doi.org/10.1016/j.saa.2019.117802
11. M.A.J. Queen, K.C. Bright, S.M. Delphine, P.A. Udhaya, Enhanced linear and non-linear optical activity of lead onto L threonine cadmium acetate crystal. J. Mater. Sci. Mater. Electron. **32**(10), 13261–13268 (2021). https://doi.org/10.1007/s10854-021-05881-y
12. M.A.J. Queen, K.C. Bright, P.A. Udhaya, Investigation on the effect of Potassium on the structural, optical and thermal properties of the L threonine cadmium acetate: elucidation of organo cadmium compound for dielectric filters. J. Mater. Sci. Mater. Electron. **34**, 181 (2023). https://doi.org/10.1007/s10854-022-09620-9
13. T. Vu, O.Y. Khyzhun, A.A. Lavrentyev, B.V. Gabrelian, K.F. Kalmykova, L.I. Isaenko, A.A. Goloshumova, P.G. Krinitsyn, G.L. Myronchuk, M. Piasecki, Electronic band structure and optical properties of Li2In2GeSe6 crystal. Mater. Today Commun. **35**, 105798 (2023). https://doi.org/10.1016/j.mtcomm.2023.105798
14. E.P. Wagner, Investigating bandgap energies, materials, and design of light emitting diodes. J. Chem. Educ. **93**, 1289–1298 (2016). https://doi.org/10.1021/acs.jchemed.6b00165
15. N. Mir, M. Salavati-Niasari, Preparation of TiO_2 nanoparticles by using tripodal tetraamine ligands as complexing agent via two-step sol–gel method and their application in dye-sensitized solar cells. Mater. Res. Bull. **48**(4), 1660–1667 (2013). https://doi.org/10.1016/j.materresbull.2013.01.006
16. M.H. Khorasanizadeh, R. Monsef, M. Salavati-Niasari, H.S. Majdi, W.K. Al-Azzawi, F.S. Hashim, Schiff-base ligand assisted synthesis of DyVO4/ AgBr nanocomposites, characterization, and investigation of photocatalytic activity over organic dye contaminants. Arab. J. Chem. **16**(8), 105020 (2023)
17. A. Panahi, R. Monsef, E.A. Dawi, A.S. Hussein, M. Salavati-Niasari, Green auto-combustion synthesis and characterization of $TmVO_4$ nanostructures in the presence carbohydrate sugars and their application as visible-light photocatalyst. Sol. Energy **258**, 372–382 (2023). https://doi.org/10.1016/j.solener.2023.04.030
18. S. Zinatloo-Ajabshir, M. Baladi, M. Salavati-Niasari, Enhanced visible-light-driven photocatalytic performance for degradation of organic contaminants using PbWO4 nanostructure fabricated by a new, simple and green sonochemical approach. Ultrason. Sonochem. **72**, 105420 (2021)
19. M.S. Javed, A.J. Khan, A. Ahmad, S.H. Siyal, S. Akram, G. Zhao, A.A.A. Bahajjaj, M. Ouladsmane, M. Alfakeer, Design and fabrication of bimetallic oxide nanonest-like structure/carbon cloth composite electrode for supercapacitors. Ceram. Int. **47**(21), 30747–30755 (2021). https://doi.org/10.1016/j.ceramint.2021.07.254
20. T.R. Kumar, M.A.J. Queen, K.C. Bright, R. Ilangovan, K. Sankaranarayanan, Investigation on the physico-chemical properties of Sodium L-alanine cadmium chloride crystal and assessment for their non linear optical response. Eur. Chem. Bull. **12**(3), 1633–1649 (2023)
21. SK Kurtz, TT Perry, A Powder technique for the evaluation of nonlinear optical materials. J. Appl. Phys. 39, 3798–3813 (1968)
22. J.D. Lee, *Concise of organic chemistry* (Wellwish Science, Germany, 2004)
23. A.K. Panigrahi, T. Ghosh, S.R.K. Vanjari, S.G. Singh, Oxidation resistive, CMOS compatible copper-based alloy ultrathin films as a superior passivation mechanism for achieving 150 °C Cu–Cu wafer on wafer thermocompression bonding. IEEE Trans. Electron Devices **64**, 1239–1245 (2017)
24. T.R. Kumar, M.A.J. Queen, K.C. Bright, R. Ilangovan, K. Sankaranarayanan, Comparative study on structural, mechanical, optical and Dielectric properties of L alanine cadmium chloride and manganese L alanine cadmium chloride crystal. Chem. Afr. **6**, 3229–3236 (2023). https://doi.org/10.1007/s42250-023-00697-1

25. P. Nisha Santha Kumari, S. Kalainathan, G. Bhagavannarayana, Study of crystalline perfection and thermal analysis of zinc cadmium thiocyanate single crystals grown in silica gel. Cryst. Res. Technol. **43**, 276–281 (2008)